Shunt capacitive switches based on VO_2 metal insulator transition for RF phase shifter applications

E. A. Casu[1], W. A. Vitale[1], M. Tamagnone[2], M. Maqueda Lopez[1], N. Oliva[1], A. Krammer[3], A. Schüler[3], M. Fernández-Bolaños[1], A.M. Ionescu[1]

[1]Nanoelectronic devices laboratory (NanoLab)
[2]Laboratory of Electromagnetics and Acoustics (LEMA)
[3]Solar Energy and Building Physics Laboratory (LESO-PB)
École Polytechnique Fédérale de Lausanne (EPFL), CH-1015 Lausanne, Switzerland
emanuele.casu@epfl.ch

***Abstract*—This paper presents a wide-band RF shunt capacitive switch reconfigurable by means of electrically triggered Vanadium Oxide (VO_2) phase transition to build a true-time delay (TTD) phase shifter. The concept of VO_2-based reconfigurable shunt switch has been explained and experimentally demonstrated by designing, fabricating and characterizing an 819 µm long unit cell. The effect of bias voltage on losses and phase shift has been studied and explained. By triggering the VO_2 switch insulator to metal transition (IMT) the total capacitance can be reconfigured from the series of two metal-insulator-metal (MIM) capacitors to a single MIM capacitor. Higher bias voltages are more effective in this reconfiguration and give a higher phase shift. The optimal achievable performance has been shown heating the devices above VO_2 IMT temperature. A maximum of 16° per dB loss has been obtained near the design frequency (10 GHz).**

Keywords—vanadium dioxide; phase transition; RF switch; true-time delay; phase shifter; tunable capacitor;

I. INTRODUCTION

Phase shifters are key components for beam-steering implementations, smart adaptive antennas and scanning applications for wideband communications and remote sensing systems. RF distributed MEMS transmission lines (DMTL) have been proven to be an interesting concept to achieve a high phase shift over a wider frequency band compared to traditional solid-state implementations (PIN diodes, GaAs FET, Ferrite materials). Nevertheless, critical issues of MEMS technology, such as reliability, process variability and packaging requirements are still a limiting factor for a widespread implementation.

Strongly correlated functional oxides exhibiting metal to insulator transition have recently emerged in research as promising materials for a large number of applications, including steep transistors [1], RF switches [2,3], reconfigurable filters [4,5] and antennas [6,7]. Vanadium Oxide (VO_2) has proven to be one of the most interesting among these materials thanks to its large change in conductivity between its two states and the possibility of achieving the phase transition by electrical excitation [8].

Compared to MEMS switches, VO_2 switches offer clear advantages such as an easier integration in microelectronic technological processes, smaller footprint and a three order of magnitude faster switching time [9]. A switched line phase shifter with thermally actuated VO_2 switches has been previously demonstrated in microstrip technology [10].

In this paper we present for the first time a shunt capacitive switch reconfigurable by means of electrically triggered VO_2 phase transition to build true-time delay phase shifters by periodically loading a coplanar waveguide (CPW) with the capacitive switches (Fig. 1). We present the concept of the device and we validate it by fabricating, designing and characterizing an 819 µm long unit, able to provide up to 16° phase shift per dB loss at 10 GHz.

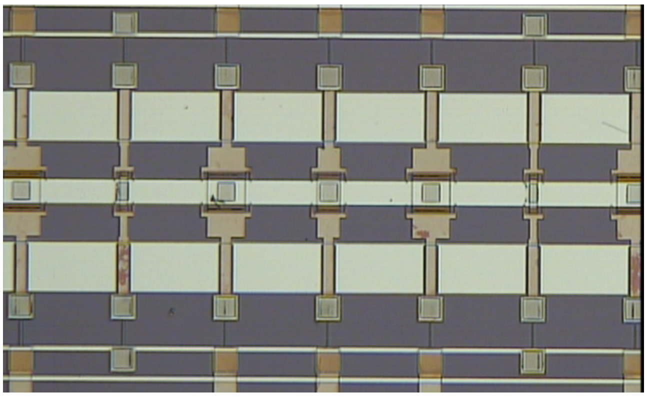

Fig. 1. Optical image of the CPW phase shifter showing the cascaded VO_2-based capacitive shunt switches designed to achieve 3-bits phase states.

II. RECONFIGURABLE CAPACITIVE SHUNT SWITCH

The reconfigurable capacitive shunt switch consists of two fixed MIM capacitors in series, C_S and C_G, where the first can be short-circuited by actuating a VO_2 two-terminal switch (Fig. 2). Below the phase-transition temperature and when no bias is applied, the VO_2 is in its insulating state so that the switch exhibits a high resistance level and can be considered open. The two capacitors are then electrically in series, offering an equivalent capacitance $C_{TOT} = C_G{*}C_S / (C_G{+}C_S)$. Whenever a bias larger than the switch actuation voltage is applied, the VO_2 film phase changes to its conductive state and the switch exhibits a low resistance value. In this case the C_S capacitor is short-circuited by the switch and the equivalent capacitance between the signal and the ground line will be simply C_G. In this way the VO_2 switch allows to reconfigure the loading capacitance between C_G and C_{TOT}.

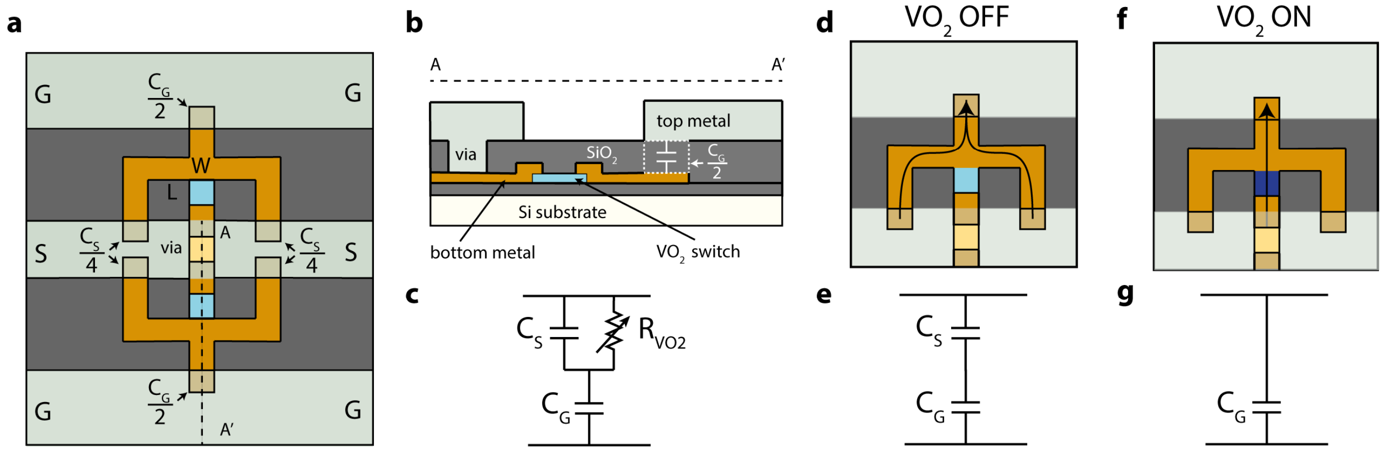

Fig. 2. a) Schematic of the reconfigurable capacitive shunt switch. A via connects the signal top metal line with ametal line underneath in contact with a VO_2 switch. Four MIM capacitor $C_S/4$, two per side, lay between the signal line and the underneath metal, whilst other two MIM capacitor $C_G/2$, one per side, lay between the ground planes and the underneath metal. b) Cross-section beween signal and ground plane highlighting the via between the two metals, the VO_2 switch and the capacitance $C_G/2$. c) Equivalent circuit of the capacitive divider, with the VO_2 switch modeled as a variable resistor R_{VO2}. d) Preferential path seen by the signal when the VO_2 is in insulating phase, with an equivalent capacitance given by the series of C_S and C_G. e) Equivalent circuit for the insulating phase, where the switch can be modeled as an open switch (R_{VO2} > 1 kΩ). f) When the VO_2 film is in its conducting phase the capacitors $C_S/4$ are short-circuited by the switch (R_{VO2} ~ 1 Ω) and g) the equivalent capacitance seen between signal and ground equals C_G.

The VO_2 switch can be electrically actuated by means of a bias line decoupled from the RF signal by means of a serpentine resistor realized with a 25 nm-thick Chromium (Cr) film. The switch resistance is in the high state until a critical power is achieved which causes a steep insulator to metal transition (Fig. 3). In order not to affect the RF performance, the length and width of the switch are chosen to be 1 µm and 30 µm respectively, so to obtain a high value of resistance in the off-state (> 1 kΩ) and low value of resistance in the on-state (~1 Ω), while keeping a reasonably low actuation voltage.

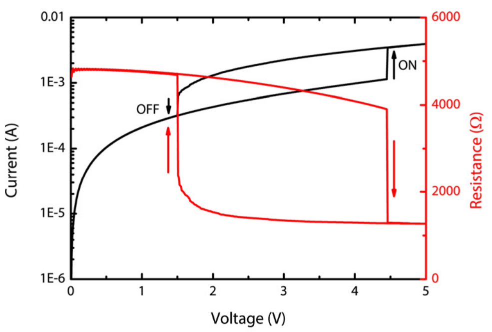

Fig. 3. Current versus voltage electrical characteristic and extracted resistance of the VO_2 switch with an integrated serpentine resisistor of 1.2 kΩ in series. The arrows indicates the insulator-metal transition and metal insulator transition.

The phase shifter was fabricated using standard microelectronics processes starting with a high-resistivity 525 µm thick silicon substrate passivated with 500 nm LPCVD-deposited SiO_2 (Fig. 4). The VO_2 film was prepared by reactive magnetron sputtering deposition starting from a Vanadium target [11]. After the deposition, a resistivity ratio higher than 3 decades was measured with a Van der Pauw measure performed at different temperatures (Fig. 5). The film was then patterned using photolithography and wet etching. The bias resistors were realized by lift-off of a 25 nm thick Cr film. A 200 nm thick Al film was subsequently deposited and patterned with lift-off to act as bottom metal. A 300 nm thick SiO_2 film was sputtered as insulating layer and as a dielectric for MIM capacitors. Vias were opened by photolithography and dry etching. A final 800 nm thick Al top metal layer was deposited to create the CPW and the contacts on the bottom metal bias lines.

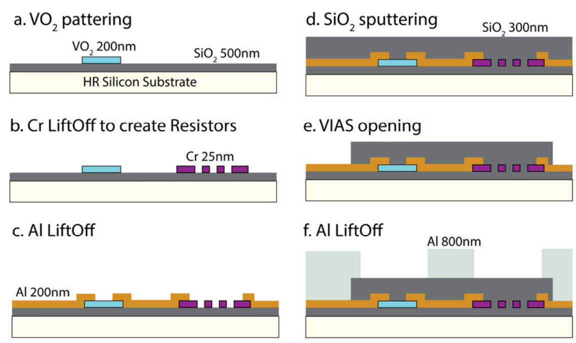

Fig. 4. Fabrication process of the capacitive shunt switch with VO_2 switches and integrated bias resistors.

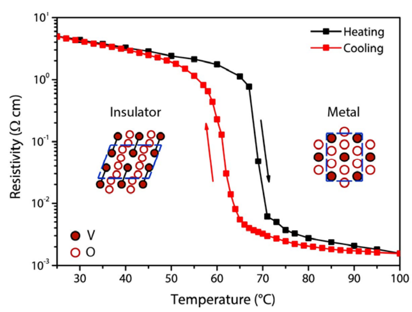

Fig. 5. Dependence of resistivity on temperature for the deposited 200 nm thick VO_2 film.

III. Unit Cell Performance

The CPW was designed with a signal width of 100 µm and a ground plane spacing of 150 µm to obtain an unloaded waveguide impedance of 65 Ω. The design of the unit cell for the phase shifter was done following the method described in [12] in order to maximize the phase shift for the minimum insertion loss (IL). Starting from the chosen values of impedances in the ON and OFF state, respectively $Z_{ON} = 42\ \Omega$ and $Z_{OFF} = 58\ \Omega$, and having chosen the Bragg frequency to be three times the frequency of design for the phase shifter, for a design frequency of 10 GHz the unit cell length was calculated to be 819 µm. The computed capacitances were $C_{ON} = 143$ fF and $C_{OFF} = 26$ fF resulting in a capacitance ratio of 5.5. Thus the MIM capacitances for the reconfigurable capacitive shunt switch are calculated as $C_S = 31.7$ fF and $C_G = 143$ fF.

The device was characterized by using an Anritsu VectorStar MS4647B Vector Network Analyser to measure *S*-parameters, a HP 4155B Semiconductor Parameter Analyser to provide the bias to operate the VO_2 switches and a Cascade Summit prober with a thermo-chuck to control the substrate temperature.

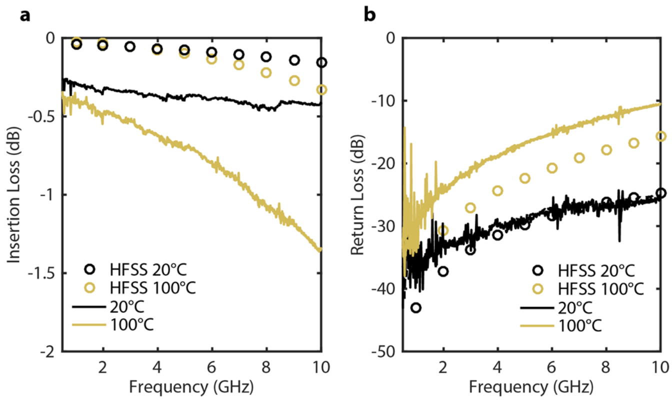

Fig. 6. (a) Insertion Loss and (b) Return Loss of the measured unit cell at 20 °C and 100 °C. Circles correspond to ANSYS HFSS simulations. The simulations have been performed using the VO_2 resistivity measured at 20 °C for the OFF state and 100 °C for the ON state.

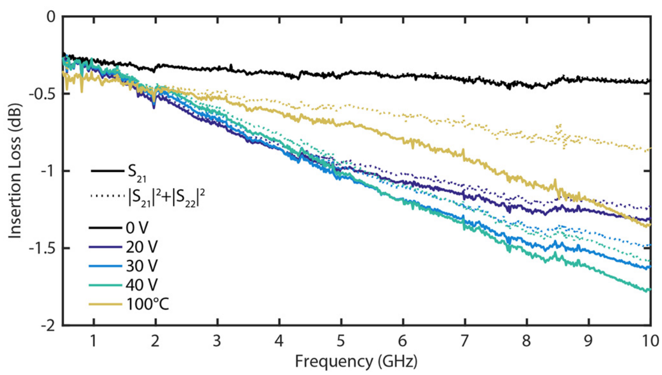

Fig. 7. Insertion loss (continuous lines) and no-reflection losses (dotted lines) versus frequency, measured at 20 °C substrate temperaure for 0 V, 20 V, 30 V and 40 V bias voltage and at 100 °C with no applied bias.

Fig. 6 shows comparison between Ansys HFSS simulations of *S*-parameters and measurements with no bias at 20°C (OFF state) and 100°C (ON state), well above the phase transition temperature where the VO_2 film becomes fully conductive (see Fig. 5). When the switches are turned off (20 °C and no bias) the insertion loss is 0.43 dB at 10 GHz, while in the ON state the insertion losses are increased both in simulation and measurements. The difference between measured and simulated values could be attributed to resistive losses along the line and in the VO_2 switch for the ON state.

The devices were measured for different bias values above the actuation voltage of the VO_2 switches (Fig. 7). While the insertion loss seems to increase by increasing the bias, the loss at the design frequency is improved when the switch is at its lowest possible resistance value, obtained measuring at 100 °C. This behavior can be explained looking at the losses not due to reflection. While in the OFF state the insertion losses and no-reflection losses are almost coincident, indicating a good match, in the ON state the behavior varies depending on the bias. At 20 V the IL and total losses are similar, while at 30 V and 40 V a considerable part of the IL is due to the mismatch. At 100 °C the IL are lower than at the considered bias points and the no-reflection losses are minimized, showing better accordance with the FEM simulations.

The measured phase shift with respect to the OFF state increases with the applied bias but tends to saturate around 5 GHz for 40 V bias, while at 100 °C it is linear over the considered frequency band (Fig. 8). The phase shift per dB loss shows as well that the best trade-off is obtained for higher bias and indicates that best performances are obtained at 100 °C, where a maximum of 16° per dB loss is obtained slightly below the design frequency.

The limited performance of the device when electrically actuated suggests that for the used bias voltages, the conduction channel in the VO_2 switch does not extend to the entire film width [13] and its resistance is still not low enough to grant a full capacitance reconfiguration and to prevent significant RF losses. We can assume that by applying a larger bias voltage and thus by injecting a larger current the performances will converge to the one measured at 100 °C.

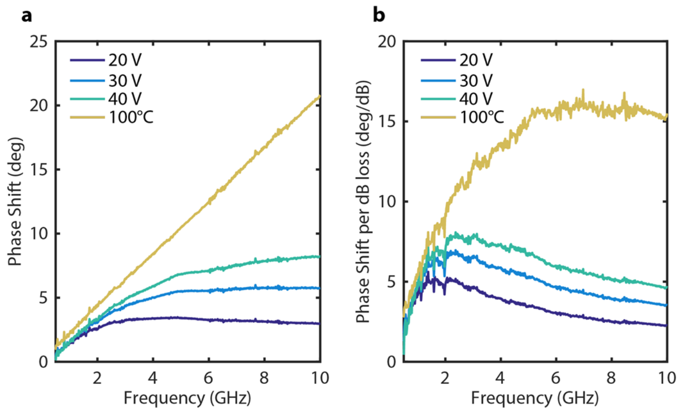

Fig. 8. (a) Phase shift and (b) phase shift per dB loss extracted from *S*-parameter measurements at 20 °C for 0 V, 20 V, 30 V and 40 V bias voltage at and at 100 °C with no applied bias.

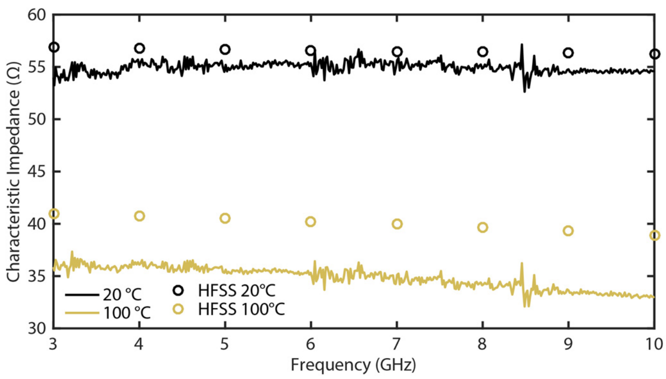

Fig. 9. Equivalent characteristic impedance of the unit cell, extracted from measures at room temperature and at 100 °C (solid lines), and from ANSYS HFSS simulations (symbols).

The equivalent impedance of the loaded line was calculated using the method proposed in [14] and is shown in Fig. 9. In the OFF state the equivalent impedance is about 55 Ω at 10 GHz, not far from the simulated value of 56 Ω. In the ON state at 100 °C the measured impedance is lower than the simulated one, in accordance with the larger measured phase shift and larger insertion loss due to reflection.

IV. PHASE SHIFTER

In order to predict the performance of a phase shifter, the measured *S*-parameters in OFF and ON states (20 and 100 °C temperature) of the unit cell were mathematically cascaded to consider the presence of more stages in series. The predicted performance of a 6-stages phase shifter targeting 120° shift at 10 GHz is shown in Fig. 10. In order to actuate the different stages it is possible to use multiple bit lines that actuate group of switches to achieve the desired phase shift.

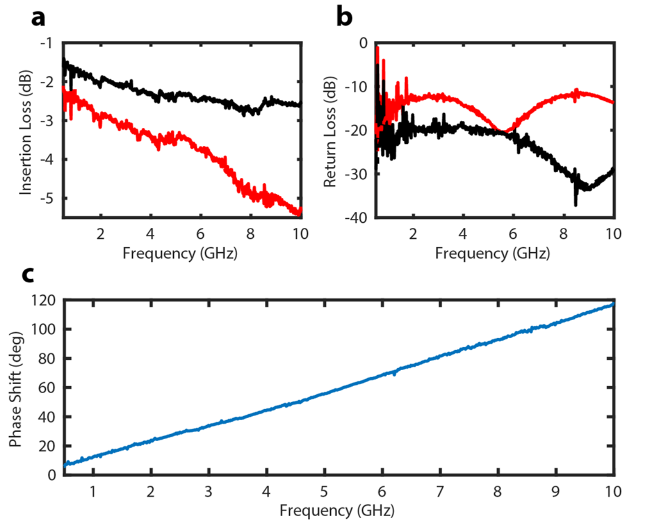

Fig. 10. Predicted (a) insertion loss, (b) return loss and (c) phase shift for a 6-stage phase shifter.

V. CONCLUSION

This paper reports for the first time a VO_2-based capacitive shunt switch as a building block to be cascaded to obtain TTD phase shifters. The working principles as well as the fabrication method have been presented and validated by designing, fabricating and characterizing a unit cell. Insertion losses, largely due to mismatch could be easily reduced by tuning MIM capacitor design. The measurements at different bias voltage and at high temperature have revealed the need of a better optimization of the VO_2 switch in order to have lower resistance values in the ON state to match the good performances at high temperatures. Nevertheless the VO_2-based reconfigurable capacitive switches offer a unique opportunity to build ultrafast and reliable phase shifters.

ACKNOWLEDGMENT

This work has been supported by the ERC Advanced Grant ‘Millitech’ of the European Commission, the Swiss National Science Foundation (Grant No. 144268) and the Swiss Federal Office of Energy (Grant No. 8100072).

REFERENCES

[1] E. A. Casu et al., “Hybrid phase-change — Tunnel FET (PC-TFET) switch with subthreshold swing < 10mV/decade and sub-0.1 body factor: Digital and analog benchmarking,” in *2016 IEEE International Electron Devices Meeting (IEDM)*, 2016, p. 19.3.1-19.3.4. doi:10.1109/IEDM.2016.7838452

[2] S. D. Ha, Y. Zhou, C. J. Fisher, S. Ramanathan, and J. P. Treadway, “Electrical switching dynamics and broadband microwave characteristics of VO2 radio frequency devices,” *J. Appl. Phys.*, vol. 113, pp. 1–25, 2013.

[3] W. A. Vitale et al., “Steep slope VO2 switches for wide-band (DC-40 GHz) reconfigurable electronics,” in *72nd Device Research Conference*, 2014, pp. 29–30. doi:10.1109/DRC.2014.6872284.

[4] D. Bouyge and A. Crunteanu, “Applications of vanadium dioxide (VO2)-loaded electrically small resonators in the design of tunable filters,” in *European Microwave Conference, 2010*, 2010, no. September, pp. 822–825..

[5] W. A. Vitale et al., “Electrothermal actuation of vanadium dioxide for tunable capacitors and microwave filters with integrated microheaters,” *Sensors Actuators A Phys.*, vol. 241, pp. 245–253, Apr. 2016.

[6] T. Teeslink, D. Torres, J. Ebel, N. Sepulveda, and D. Anagnostou, “Reconfigurable Bowtie Antenna using Metal-Insulator Transition in Vanadium Dioxide.,” *IEEE Antennas Wirel. Propag. Lett.*, vol. 1225, no. c, pp. 1–1, 2015.

[7] W. A. Vitale et al., “Modulated scattering technique in the terahertz domain enabled by current actuated vanadium dioxide switches,” *Sci. Rep.*, vol. 7, no. December 2016, p. 41546, 2017.

[8] Z. Yang, C. Ko, and S. Ramanathan, “Oxide Electronics Utilizing Ultrafast Metal-Insulator Transitions,” *Annu. Rev. Mater. Res.*, vol. 41, no. 1, pp. 337–367, Aug. 2011.

[9] J. Leroy et al., “High-speed metal-insulator transition in vanadium dioxide films induced by an electrical pulsed voltage over nano-gap electrodes,” *Appl. Phys. Lett.*, vol. 100, no. 21, p. 213507, 2012.

[10] C. Hillman and P. Stupar, “An ultra-low loss millimeter-wave solid state switch technology based on the metal-insulator-transition of vanadium dioxide,” *Microw. Symp. Dig. IEEE MTT-S Int.*, pp. 0–3, 2014.

[11] W. A. Vitale et al., “Fabrication of CMOS-compatible abrupt electronic switches based on vanadium dioxide,” *Microelectron. Eng.*, vol. 145, pp. 117–119, Sep. 2015.

[12] G. M. Rebeiz, “RF MEMS: theory, design, and technology,” *John Wiley & Sons, 2004.*

[13] J. Yoon et al., “Investigation of length-dependent characteristics of the voltage-induced metal insulator transition in VO 2 film devices,” *Appl. Phys. Lett.*, vol. 105, no. 8, p. 83503, Aug. 2014.

[14] J. Perruisseau-Carrier et al., “Modeling of periodic distributed MEMS - Application to the design of variable true-time delay lines,” *IEEE Trans. Microw. Theory Tech.*, vol. 54, no. 1, pp. 383–392, 2006.